A climate index for the Newfoundland and Labrador shelf

Frédéric Cyr[1,2] and Peter S. Galbraith[3]

[1]Northwest Atlantic Fisheries Centre, Fisheries and Oceans Canada, St. John's, NL, Canada
[2]Memorial University of Newfoundland, St. John's, NL, Canada
[3]Maurice Lamontagne Institute, Fisheries and Oceans Canada, Mont-Joli, QC, Canada

Correspondence: Frédéric Cyr (Frederic.Cyr@dfo-mpo.gc.ca)

Abstract. This study presents in detail a new climate index for the Newfoundland and Labrador (NL) shelf. The NL climate index aims to describe the environmental conditions on the NL shelf and in the Northwest Atlantic as a whole. It consists of annual normalized anomalies of 10 subindices with equal contribution: Winter North Atlantic Oscillation, air temperature, sea ice season severity, iceberg count, sea surface temperature, vertically-averaged temperature and salinity at the Atlantic Zone

5 Monitoring Program (AZMP) Station 27, cold intermediate layer (CIL) core temperature at AZMP Station 27, CIL area on 3 AZMP hydrographic sections and bottom temperature on the NL shelf. This index runs from 1951 to 2019 and will be updated annually. This index and the subindices are available at https://doi.org/10.20383/101.0301 (Cyr and Galbraith, 2020).

1 Introduction

Climate indices are often regarded as simple ways to relate the mean environmental conditions to the state of an ecosystem. In

10 Newfoundland and Labrador (NL), climate indices are often used by Fisheries and Oceans Canada (DFO) to inform fisheries scientists and managers as part of various regional assessment processes of fisheries resources and ecosystem studies (e.g., Koen-Alonso et al., 2010; NAFO, 2017, 2018; DFO, 2020b; Hammill et al., 2020; Stenson et al., 2020). A new version of the climate index or the NL shelf is introduced here. It replaces the Composite Environmental Index (CEI) developed by Petrie et al. (2007), and used until recently in annual reports on the physical oceanographic and meteorological conditions on the NL

15 shelf (e.g., Colbourne et al., 2017; Cyr et al., 2019). This new index was introduced by Cyr et al. (2020) but is detailed here for the first time. At the moment, this index runs from 1951 to 2019, but will be updated annually (see data availability).

2 Climate index components

The NL climate index aims to represent the large-scale climate conditions and state of the physical environment on the NL shelf and the Northwest Atlantic in general (see Figure 1 for map). The index is a composite of 10 components (or subindices)

20 estimated annually by DFO (e.g. Cyr et al., 2020). These subindices are presented in the following sub-sections.

The climate index and most subindices start in 1951. Prior to 1951, there are too few observations for many of subindices to achieve a level of accuracy and precision that would provide high confidence in their estimates. Except for the North Atlantic Oscillation (NAO), these sub-indices are presented in terms of normalized anomalies ($\tilde{X}$):

$$\tilde{X} = \frac{X - \overline{X}_{\text{clim}}}{sd(X)_{\text{clim}}}, \tag{1}$$

25 where X represents any annual time series, and $\overline{X}_{\text{clim}}$ and $sd(X)_{\text{clim}}$ are the average and standard deviation of X over the climatological period. Unless otherwise specified, the climatological period is 1981-2010, according to the international standards (World Meteorological Organization, 2017). This climatological period will be updated to 1991-2020 during the next annual update of the index.

2.1 North Atlantic Oscillation

30 The North Atlantic Oscillation (NAO) refers to the anomaly in the sea-level pressure (SLP) difference between the sub-tropical high (near the Azores) and the subpolar low (near Iceland). While several operational definitions of the NAO exist, the monthly NAO based on empirical orthogonal functions from Hurrell (1995) is used here. This definition better represents the larger-scale influence of the SLP patterns above the Northwest Atlantic, and tends to be less noisy than the station-based definition. This time series is available online via the National Center for Environmental Information of the National Oceanic and Atmospheric 35 Administration (https://www.ncdc.noaa.gov/teleconnections/nao/). This index is a normalized anomaly by construction and is not re-normalized here.

The winter NAO, defined as the average of monthly values from December to March, is considered here (Figure 2). A positive phase of the NAO index is usually associated with an intensification of the Icelandic Low and the Azores High SLP. Except for some years for which the SLP patterns are spatially shifted (e.g., 1999, 2000 and 2018), positive winter NAO years 40 usually favor strong Northwesterly winds, cold air and cold sea surface temperatures, and heavy ice conditions in the Northwest Atlantic (Colbourne et al., 1994; Drinkwater, 1996; Petrie et al., 2007). A predominance of strongly positive winter NAO phase has persisted since 2012, including the record high of +1.61 in 2015 (the record low of -1.47 was in 2010). This recent positive phase of the NAO also corresponded to an intensification of the convection in the Labrador Sea (Yashayaev and Loder, 2017).

2.2 Air Temperature

45 The air temperature subindex consists of the annual normalized anomalies at five coastal communities around the Northwest Atlantic: Nuuk (Greenland), Iqaluit (Baffin Island), Cartwright (Labrador) and Bonavista and St. John's in Newfoundland (see Figure 1). While the data for Nuuk are obtained from the Danish Meteorological Institute (Vinther et al., 2006), the air temperature data from Canadian sites are from the second generation of Adjusted and Homogenized Canadian Climate Data (AHCCD) that accounts for shifts in station location and changes in observation methods (Vincent et al., 2012). When 50 necessary, they are updated using Environment Canada's National Climate Data and Information Archive.

Annual normalized anomalies since 1951 for these five sites are presented in Figure 3 under the form of a stacked bar plot. While 1972 appears as the coldest year of this time series, the period of the early 1990's exhibits a sustained period of cold air temperature, with 1991, 1992 and 1993 being respectively the sixth, second and third coldest years of the entire time series. This cold period was followed by the predominance of warmer-than-normal air temperatures at all sites from the mid-1990s to

55   about 2013, with 2010 being the warmest year on record by a large extent. Except for 2015, which was the coldest year since 1993, recent years were close to normal.

2.3   Sea Ice

Sea ice season duration and maximum cover area are estimated from ice cover products obtained from the Canadian Ice Service (CIS). The methodology is described in (Galbraith et al., 2020) and briefly summarized here. The source CIS products consist

60   of weekly Geographic Information System (GIS) charts covering the East coast for the period 1969-2019 and Hudson Bay for the period 1980-2019. The Hudson Bay charts include coverage of the Northern Labrador Shelf and the East coast charts cover the Southern Labrador Shelf as well as the Newfoundland Shelf (Figure 1). For each of the three regions, the seasonal maximum area of sea ice was determined as well as the ice season duration (Figure 4). The former accounts for partial coverage (as opposed to sea ice extent) and the latter is obtained from a spatial average of the number of weeks with sea ice at every

65   pixel, with zeros counted for areas where no ice was present but the 30 year climatology shows some. These 6 times series (two variables over three regions) are then combined into mean normalized anomalies and presented in a stacked bar plot (Figure 4, bottom panel). The annual average of the normalized anomalies is also presented in a color-coded scorecard at the bottom of this panel. Negative anomalies, indicative of warmer conditions, have been colored red, and positive anomalies blue. This time series corresponds to the sea ice contribution to the NL climate index. The periods of maximum sea ice cover and season

70   duration are found in the early 1970's, mid-1980's and early 1990's. Since the early 1990's the severity of the sea ice season has gradually decreased, reaching the lowest values in 2011 and 2010. With the exception of a rebound to near-normal values in 2014-2016, sea ice conditions have been weak over recent years.

2.4   Iceberg count

The number of icebergs drifting south of 48°N in the Northwest Atlantic has been monitored by the International Ice Patrol of

75   the US Coast Guard since 1900 (International Ice Patrol, 2020). The entire time series is presented in Figure 5. The 120-year average annual number is 498 and the 1981-2010 average is 767. An iceberg count above 1500 has been observed in some years, including in 2014, 2019, and between the early-1980s and mid-1990s. The all-time record of 2202 was reached in 1984. Only 2 years (1966 and 2006) in the 120-year time series reported no icebergs south of 48ºN. Years with low iceberg numbers on the Grand Banks generally correspond to higher than normal air temperatures, lighter than normal sea-ice conditions, and

80   warmer than normal ocean temperatures on the NL Shelf. The normalized anomalies of this time series since 1951 corresponds to the icebergs contribution to the NL climate index. The latter is provided under the form of a scorecard below the main panel of Figure 5.

2.5 Sea Surface Temperature

Sea Surface Temperatures (SSTs) used here are a blend of data from Pathfinder version 5.3 (1982-2019), Maurice Lamontagne
Institute (1985-2013) and Bedford Institute of Oceanography (1997-2019). Monthly anomalies are computed as the average
of available daily anomalies at the pixel level within each geographical region, chosen to be the NAFO Divisions of Figure 1,
except that here they are cropped at the shelf break. Details of the processing are in Galbraith et al. (2020) with the extended
spatial coverage as in DFO (2020a). The climatological reference period for SST is 1982-2010.

Figure 6 presents annual normalized anomalies averaged over the ice-free season, where the contribution of each region is
weighted according to its open water area. The ice-free season varies from as short as June to September in NAFO Division
2G, to as long as March to November in NAFO Division 3P (seasonal information in the legend of Figure 6). This time series
correspond to the SST contribution to the NL climate index (normalized anomalies are color-coded at the bottom of the figure).
This figure shows the colder than average conditions that prevailed in the early 1990's, with 1991 and 1992 being the coldest
years of this time series. This period was followed by a predominance of warmer than average conditions that lasted until about
2015. In recent years, 2018 and 2019 were colder than normal (defined as $\tilde{\mathrm{SST}} < -0.5\,\mathrm{sd}$; or blue colors at the bottom of
Figure 6). These are the first colder than normal conditions since 1995.

2.6 Station 27 data

Station 27 (47° 32.8'N; 52° 35.2'W) is located in the Avalon Channel just outside St. John's harbour, NL (Figure 1). It is
one of longest hydrographic time series in Canada with frequent (near-monthly basis) conductivity-temperature-depth (CTD)
observations since 1946. Station 27 was integrated into DFO's Atlantic Zone Monitoring Program (AZMP, Therriault et al.,
1998) in 1999. In addition to sampling during these traditional hydrographic surveys, this station has been seasonally equipped
with an automatic CTD profiling system installed on a surface buoy (type Viking) since 2017 (see Cyr et al., 2020, for further
information).

Station occupations were first combined into monthly averaged temperature (T) and salinity (S) profiles from which the
climatological annual cycle was extracted (Figure 7). This figure shows the seasonal warming of the top layer (∼20 m), with
temperature peaking in August before being mixed during the fall (top panel). Also visible in the temperature field is the cold
intermediate layer (CIL), a prominent feature of the NL ecosystem (Petrie et al., 2007). The CIL is defined here as the water
below 0°C and delineated with thick black contour in the top panel of Figure 7. This layer originates in the winter as a cold
surface layer, which becomes isolated from the surface after the apparition of a seasonally heated surface layer during the spring
(April-May). The CIL thus remains below the surface throughout most of the year, while its top boundary slowly deepens from
about 50 to 100 m as the heat from the surface layer penetrates deeper into the water column. While in deeper areas of the NL
shelf a third warmer layer is present beneath the CIL, at Station 27 the CIL generally extend down to the bottom (∼176 m). The
summer CIL core temperature is defined as the minimum temperature of the monthly mean profile between June and August
(see below).

115   The surface salinity at Station 27 is generally lowest (S<31) between early-September and mid-October (Figure 7, bottom panel). These low near-surface salinities, generally from early summer to late fall, are prominent features of the salinity cycle on the Newfoundland Shelf and are largely due to the melting of coastal sea-ice upstream and carried over by the Labrador coastal current. Below the surface, the salinity at any depth increases in the spring and peaks in the summer before decreasing in the fall as a consequence of vertical mixing.

120   The data from Station 27, including the recent greater coverage obtained from Viking buoy automatic casts, contribute to three subindices of the NL climate index: vertically-averaged T and S, and the CIL core temperature (Figure 8). The focus here is on the period starting in 1951 for which the seasonal coverage includes at least 8 months per year. Averages from 1980 and 1981 are excluded because of insufficient seasonal coverage (4 and 7 months, respectively). In order to account for possible changes in seasonal coverage, the annual anomalies have been calculated as the averaged of monthly normalized anomalies.

125   The vertically-averaged (0-176 m) temperature exhibits decadal-like cycles (top panel). The period between the mid-1980's and mid-1990's struck as the coldest decade of the last 70 years. It was followed by a gradual warming trend that lasted two decades and peaked in 2011, the warmest year of this time series. The period from the mid-1960's and the early-1970's was also marked by sustained warmer than normal temperatures. The end of this period coincided with the freshest anomaly on record at Station 27 observed in 1970 (center panel), an event coinciding with the Great Salinity Anomaly in the North Atlantic

130   (Dickson et al., 1988). Similarly, the recent warmer than normal period (2010-2013) was followed by the second freshest anomaly on record observed in 2018. The saltiest anomaly at Station 27 (1990) on the contrary occurred during the cold period of the late-1980's and early 1990's.

The CIL subindex of Station 27 is also presented in Figure 8 (bottom panel). This time series is the average normalized anomalies of the summer (June-August) CIL core temperature (minimum temperature of the monthly mean profile). The

135   striking feature in this figure is the anomalously warm CIL anomaly present from the early 1960s to the mid-1970s. This anomaly is accentuated by the fact that the climatological reference period (1981-2010) encompasses a rather cold period that spanned the mid-1980s to the mid-1990s. After the prevalence of a warm CIL in the early 2010's (with 2010 and 2011 being the warmest years since the 1970), there has been a recent period of return to near normal conditions (roughly 2014-2017) that receded in 2018 and 2019.

140   **2.7   Cold Intermediate Layer on the NL Shelf**

As mentioned above, the CIL is a prominent feature of the NL shelf. It is found almost everywhere in subsurface during the summer. In order to highlight the influence of the CIL on the shelf as a whole, a proxy for its volume is established using the area (in km^2) of water below 0°C along Seal Island (SI), Bonavista (BB) and Flemish Cap (FC) hydrographic sections (Figure 1). These sections were selected because they have been systematically surveyed since the early 1950's before being

145   formerly standardized by the International Commission for the Northwest Atlantic Fisheries in 1976 (ICNAF, 1978). Since 1999, these hydrographic sections have been monitored by DFO as part of the AZMP.

Figure 9 shows the summer temperature along SI section during two extreme years, the warm 1965 and the cold 1990. The 1981-2010 climatology is also presented. For each sampled summer, the CIL area (e.g. the area of the section delimited by

the thick black contour in Figure 9) was calculated. For example, in 1990, the area of the CIL was $26.9\,\mathrm{km}^2$, while it was only $1.5\,\mathrm{km}^2$ in 1965. This shows the amplitude of the interannual variability of the CIL and its potential influence on the ecosystem. In 1990, most of the sea floor along SI section was in direct contact with the CIL. In 1965, when the CIL was small and fragmented, none of the sea floor was in contact with it, and the bottom conditions were in consequence several degrees warmer than in 1990.

The normalized anomalies of the CIL area for sections SI, BB and FC are presented in Figure 10. This figure highlights again the warmer conditions (negative anomalies) of the 1960's and the colder conditions of the mid-1980's and early 1990's. The average of the normalized anomalies are shown in a scorecard at the bottom of the main panel and correspond to the CIL area contribution to the NL climate index.

2.8 Bottom Temperature

Canada has been conducting random stratified trawl surveys in NAFO sub-areas 2 and 3 of the NL shelf since 1971 (Doubleday, 1981). Since 1980, temperature (and salinity since 1990) are available for most of these fishing sets thanks to trawl-mounted CTDs. The scientific trawl surveys target NAFO Subdivision 3Ps (south coast of Newfoundland) and Divisions 3LNO (Grand Banks) during the spring surveys, and Divisions 2H (northern Labrador), 2J (southern Labrador), 3K (eastern Newfoundland) and 3LNO (Grand Banks) during the fall (see map Figure 1). These surveys, combined with other available data from multiple sources (see below), are used to provide large spatial-scale oceanographic information of the NL shelf, including information on the bottom habitat parameters of numerous commercial species (e.g. Cyr et al., 2020).

The method used to derive the bottom temperature was introduced by Cyr et al. (2019) and briefly summarized here. First, all available annual profiles of temperature (scientific trawl surveys, AZMP hydrographic campaigns, surveys from other DFO regions, international oceanographic campaigns, expendable bathy-thermographs, Argo program, etc.) are vertically averaged in 5m bins and vertically interpolated to fill missing bins. Then, for each season (April-June for spring and September-December for fall), all data are averaged on a regular 0.1° x 0.1° (latitudinal x longitudinal) grid to obtain one seasonal profile per grid cell. Since this grid has missing data in many cells, each depth level is horizontally linearly interpolated. For each grid point deeper than 10 m, the bottom observation is considered as the data at the closest depth to the GEBCO 2014 Grid bathymetry (version 20141103), to a maximum 50 m difference. In order to only focus on the shelf, observations deeper than 1000 m are clipped. This method is applied for all years between 1980 and 2019 from which the 1981-2010 climatology is derived. In order to match the scientific trawl survey schedule, the normalized anomalies of bottom temperature are calculated separately for NAFO Divisions 3Ps and 3LNO in the spring, and 2H, 2J, 3K and 3LNO in the fall. The time series of the bottom temperature for both seasons is presented in a stacked bar plot in Figure 11. This figure shows the cold phase from the mid-1980's to the mid-1990's, followed by a warmer phase that peaked in 2011. A scorecard at the bottom of this figure presents the mean normalized anomalies. The latter corresponds to the bottom temperature contribution to the NL climate index.

3   NL Climate Index

Figure 12 presents, in a stacked bar plot fashion, the 10 subindices of the NL climate index previously discussed. Note that the sign of some subindices have been reversed such that a positive subindex corresponds to warm conditions (see figure caption). Since the different components do not all start in 1951, the NL climate index is defined as the averaged of the 10 components. In Figure 12, the contribution of each subindex to the average is represented by the relative length of each stacked bars. The NL climate index and its 10 subindices are provided in the data set that accompany this study (see data availability).

This NL climate index highlights the different regimes prevailing on the NL shelf and the Northwest Atlantic since 1951. For example, the 1960's stands out as the warmest decade of the entire 1951-2019 period, although it is heavily driven by CIL anomalies. The following few decades have been gradually cooling until the early 1990's, with 1991 being the coldest year on records since 1951. The warming trend that followed the early 1990's peaked in 2010-2011 (depending on the record) and was followed by recent cooling that culminated in 2015. This recently observed cold period on the NL shelf (roughly 2014-2017) was the coldest period since the early 1990's (Cyr et al., 2020) and coincided with the intensification of convection in the Labrador Sea that created the largest volume of Labrador Sea Water since the early 1990's (Yashayaev and Loder, 2017).

The correlations among the different subindices are presented in Figure 13. This shows the interactions between the different components of the climate index, while giving insights on the functioning of the NL shelf climate. The vertically-averaged temperature at Station 27 is well correlated with the bottom temperature on the NL shelf ($r = 0.82$) and with the core temperature of the CIL ($r = 0.72$). The temperature at Station 27 is also negatively correlated with sea ice ($r = -0.78$). This is because the harshness of the winter has a direct consequence on the sea ice production and the production of the CIL water. Because the CIL is in direct contact with the sea floor on a large portion of the NL shelf, it has a direct influence on its bottom temperature. It is thus not surprising that the bottom temperature at Station 27 is negatively correlated with the sea ice ($r = -0.82$). Finally, because the air temperature has a direct influence on both SST and sea ice, the correlation is good ($r = 0.74$ and $r = -0.68$, respectively) with these variables, even if the annual air temperature average is used (i.e., includes both winter and summer). Interestingly, the winter NAO is not well correlated with any of the variables ($r < 0.5$), except slightly with the number of icebergs ($r = +0.54$). The good correlation between Station 27 temperature and other components of the climate index adds weight to numerous studies suggesting that this station is representative of the large-scale climate of the NL shelf (e.g. Petrie et al., 1992; Colbourne et al., 1994; Drinkwater, 1996; Han et al., 2015).

Figure 13 also includes the correlation coefficients between the NL climate index and all its subindices. Except for the salinity, the correlation coefficient varies between $r = 0.58$ and $r = 0.88$, the latter being with Station 27 temperature and NL shelf bottom temperature. The absence of very strong correlation (e.g. $r > 0.90$) between the different subindices, and between any subindex and the climate index itself, shows the relative independence of the different components of the climate index, and gives confidence in the choices made for its design.

Finally, there is a good correlation ($r = 0.87$) between this new climate index and the CEI developed by Petrie et al. (2007) and used until recently (e.g., Cyr et al., 2019), ensuring continuity with previous studies using this index (Figure 14). A notable difference between the two indices, however, is that the variance of the former ($\sigma^2 = 1.2$) is larger than the one of the latter

($\sigma^2 = 0.4$; note the different vertical axis systems in Figure 14). It is likely that the lower number of components used here (10

215 relatively independent subindices) makes the new climate index more stable that the previous CEI that used 28 components

(e.g., Cyr et al., 2019).

4 Conclusions

This article describes a new climate index for the Newfoundland and Labrador shelf. This index is composed of 10 subindices representing different aspect of the NL ecosystem: NAO, air temperature, sea ice season severity, icebergs count, SST, Station

220 27 temperature, salinity and CIL core temperature, CIL area on 3 hydrographic sections, and bottom temperature on the NL shelf. It is expected that this new index will be useful for ecosystem studies, fish stock assessment and forecast models.

5 Data availability

The data presented in this study are available here: https://doi.org/10.20383/101.0301 (Cyr and Galbraith, 2020). Three comma-separated values (CSV) files are provided:

225 – *NL_climate_index.csv*: Annual values of the NL climate index.

  – *NL_climate_index_all_fields.csv*: Annual values of the 10 subindices making the NL climate indices (with some signs reversed, see Figure 12 caption). The average of these 10 subindices correspond to the NL climate index.

  – *NL_climate_index_all_fields_natural_signs.csv*: annual values of the 10 subindices making the NL climate indices in with their natural sign.

230 *Author contributions.* F. Cyr designed the study, lead the writing and calculated most of the subindices. P.S. Galbraith calculated the SST and the sea ice subindices, and participated in the writing. Both authors discussed in depth the science, technical details and the structure of this article.

Competing interests. The authors declare that no competing interests are present

Acknowledgements. This work is a contribution to the Atlantic Zone Monitoring Program (AZMP) of Fisheries and Oceans Canada (DFO).
235 The authors thank the numerous scientists, technicians, captains and crew members who participated to the sampling and analysis effort since 1951. The authors also thank Dr. Pierre Pepin, who provided comments on an early version of the manuscript.

References

Colbourne, E., Narayanan, S., and Prinsenberg, S.: Climatic changes and environmental conditions in the Northwest Atlantic, 1970-1993, ICES Journal of Marine Science Symposia, 198, 311–322, 1994.

240   Colbourne, E., J. Holden, Snook, S., Han, G., Lewis, S., Senciall, D., Bailey, W., J. Higdon, and Chen, N.: Physical Oceanographic Conditions on the Newfoundland and Labrador Shelf during 2016, DFO Can.Sci. Advis. Sec. Res. Doc., 2017/079, v + 50 p., 2017.

Cyr, F. and Galbraith, P. S.: Newfoundland and Labrador climate index, https://doi.org/10.20383/101.0301, 2020.

Cyr, F., Colbourne, E., Holden, J., Snook, S., Han, G., Chen, N., Bailey, W., Higdon, J., Lewis, S., Pye, B., and Senciall, D.: Physical Oceanographic Conditions on the Newfoundland and Labrador Shelf during 2017, DFO Can.Sci. Advis. Sec. Res. Doc., 2019/051, iv +

245   58 pp., 2019.

Cyr, F., Colbourne, E., Galbraith, P. S., Gibb, O., Snook, S., Bishop, C., Chen, N., Han, G., and Senciall, D.: Physical Oceanographic Conditions on the Newfoundland and Labrador Shelf during 2018, DFO Can.Sci. Advis. Sec. Res. Doc., 2020/018., iv + 48 pp., 2020.

DFO: Oceanographic conditions in the Atlantic zone in 2019, DFO Can. Sci. Advis. Sec. Sci. Advis. Rep., 2020/028, 2020a.

DFO: 2019 Status of Northwest Atlantic Harp Seals, Pagophilus groenlandicus, DFO Can. Sci. Advis. Sec. Sci. Advis. Rep., 2020/020,

250   2020b.

Dickson, R. R., Meincke, J., Malmberg, S. A., and Lee, A.: The "great salinity anomaly" in the northern North Atlantic 1968–1982, Progress in Oceanography1, 20, 103–151, 1988.

Doubleday, W.: Manual on groundfish surveys in the Northwest Atlantic, in: NAFC Sco. Coun. Studies 2, p. 56 p., 1981.

Drinkwater, K. F.: Atmospheric and oceanic variability in the northwest Atlantic during the 1980s and early 1990s, Journal of Northwest

255   Atlantic Fishery Science, 18, 77–97, https://doi.org/10.2960/J.v18.a6, 1996.

Galbraith, P. S., Chassé, J., Shaw, J.-L., Dumas, J., Caverhill, C., Lefaivre, D., and Lafleur, C.: Physical Oceanographic Conditions in the Gulf of St. Lawrence during 2019, DFO Can. Sci. Advis. Sec. Res. Doc., 2020/30, iv + 88 pp., 2020.

Hammill, M., Stenson, G. B., Mosnier, A., and Doniol-Valcroze, T.: Trends in harp seal, Pagophilus groenlandicus, abundance in the Northwest Atlantic, 1952-2019., DFO Can. Sci. Advis. Sec. Res. Doc., 2020/in pr, iv + 28 p., 2020.

260   Han, G., Colbourne, E., Pepin, P., and Xie, Y.: Statistical Projections of Ocean Climate Indices off Newfoundland and Labrador, Atmosphere-Ocean, pp. 1–15, https://doi.org/10.1080/07055900.2015.1047732, 2015.

Hurrell, J. W.: Decadal Trends in the North Atlantic Oscillation: Regional Temperatures and Precipitation, Science, 269, 676–679, https://doi.org/10.1126/science.269.5224.676, 1995.

ICNAF: List of ICNAF Standard Oceanographic Sections and Stations, ICNAF Selected Papers Number 3, pp. 109–117,

265   https://doi.org/10.1111/j.1949-8594.1914.tb16026.x, 1978.

International Ice Patrol: International Ice Patrol Annual Count of Icebergs South of 48 Degrees North, 1900 to Present, Version 1, https://doi.org/10.7265/z6e8-3027, 2020.

Koen-Alonso, M., Pepin, P., and Mowbray, F.: Exploring the role of environmental and anthropogenic drivers in the trajectories of core fish species of the Newfoundland-Labrador marine community, NAFO Scientific Council Meeting, SCR Doc. 1, 1–16 p., 2010.

270   NAFO: Report of the 10th Meeting of the NAFO Scientific Council Working Group on Ecosystem Science and Assessment (WG-ESA), Tech. Rep. NAFO SCS Doc. 17/21, Serial No. N6774, 2017.

NAFO: Report of the 11th Meeting of the NAFO Scientific Council Working Group on Ecosystem Science and Assessment (WG-ESA), Tech. Rep. NAFO SCS Doc. 18/23, Serial No. N6900, Dartmouth, N.S., 2018.

Petrie, B., Loder, J., Lazier, J., and Akenhead, S.: Temperature and salinity variability on the eastern Newfoundland shelf: The residual field, Atmosphere-Ocean, 30, 120–139, https://doi.org/10.1080/07055900.1992.9649433, 1992.

Petrie, B., Pettipas, R. G., and Petrie, W. M.: An Overview of Meteorological, Sea Ice and Sea-Surface Temperature Conditions off Eastern Canada during 2006, Canadian Science Advisory Secretariat, 2007/022, iv + 38pp., 2007.

Stenson, G. B., Haug, T., and Hammill, M. O.: Harp Seals: Monitors of Change in Differing Ecosystems, Frontiers in Marine Science, 7, https://doi.org/10.3389/fmars.2020.569258, 2020.

Therriault, J., Petrie, B., Pepin, P., Gagnon, J., Gregory, D., Helbig, J., Herman, A., Lefaivre, D., Mitchell, M., Pelchat, B., Runge, J., and Sameoto, D.: Proposal for a northwest zonal monitoring program, Canadian Technical Report of Hydrographic and Ocean Sciences, 194, vii + 57 p., 1998.

Vincent, L. A., Wang, X. L., Milewska, E. J., Wan, H., Yang, F., and Swail, V.: A second generation of homogenized Canadian monthly surface air temperature for climate trend analysis, Journal of Geophysical Research, 117, https://doi.org/10.1029/2012JD017859, 2012.

Vinther, B. M., Andersen, K. K., Jones, P. D., Briffa, K. R., and Cappelen, J.: Extending Greenland temperature records into the late eighteenth century, Journal of Geophysical Research, 111, https://doi.org/10.1029/2005JD006810, 2006.

World Meteorological Organization: WMO guidelines on the calculation of climate normals, Tech. rep., Geneva, Switzerland, 2017.

Yashayaev, I. and Loder, J. W.: Further intensification of deep convection in the Labrador Sea in 2016, Geophysical Research Letters, 44, 1429–1438, https://doi.org/10.1002/2016GL071668, 2017.
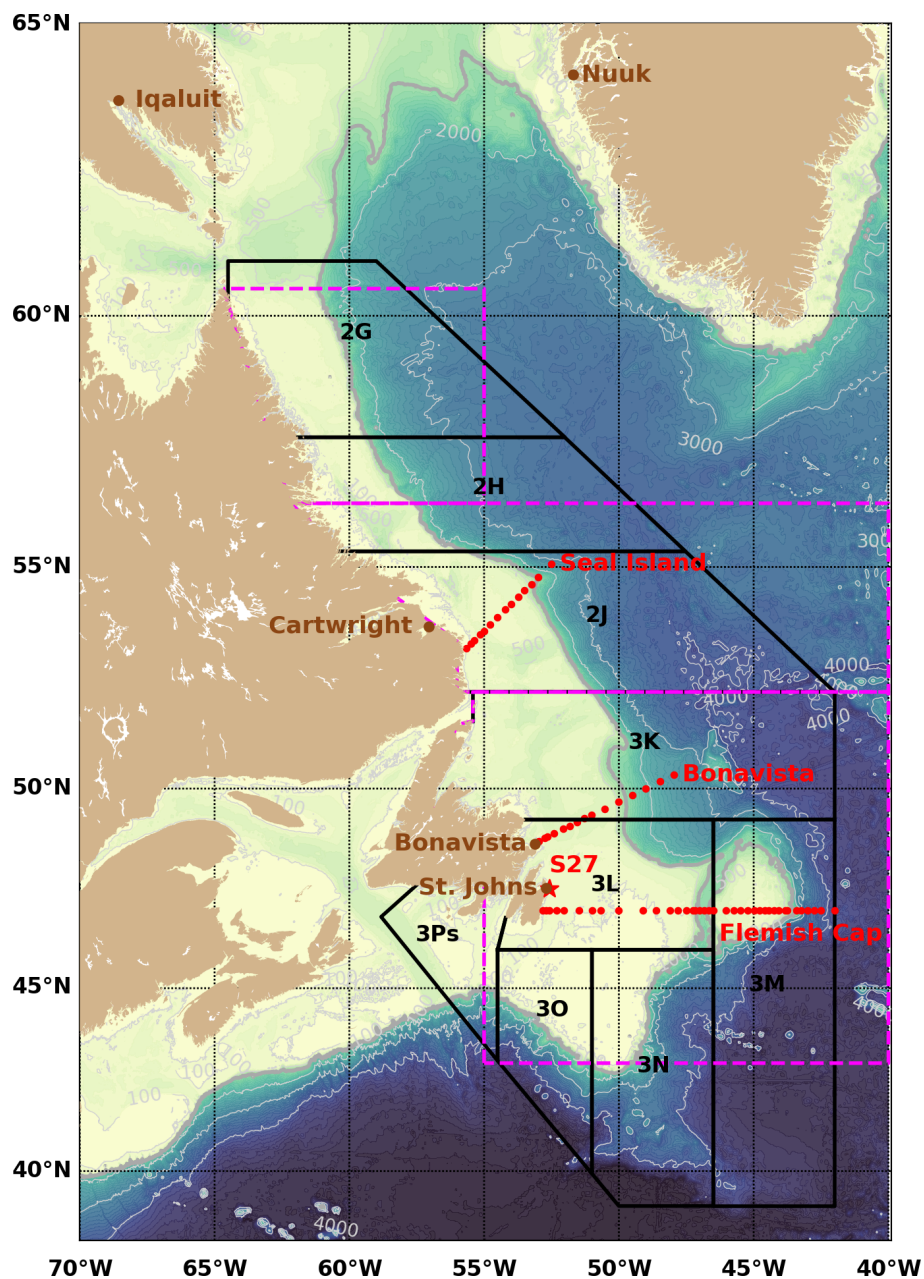
Figure 1. Map and main bathymetric features of the Northwest Atlantic ocean. NAFO Divisions (sub-areas 2 and 3) on the Newfoundland and Labrador (NL) shelf are drawn. The AZMP hydrographic sections Seal Island, Bonavista and Flemish Cap are are shown with red dots. Long-term AZMP hydrographic Station 27 is highlighted with red star. The five stations used for the air temperature time series are shown in brown. The 3 regions used for sea ice calculations are drawn with dashed magenta lines: Northern Labrador shelf, Southern Labrador shelf and Newfoundland shelf, respectively from north to south. The shelf break is delimited by a thicker and darker contour corresponding to the isobath 1000 m (used to clip the SST and bottom temperature).
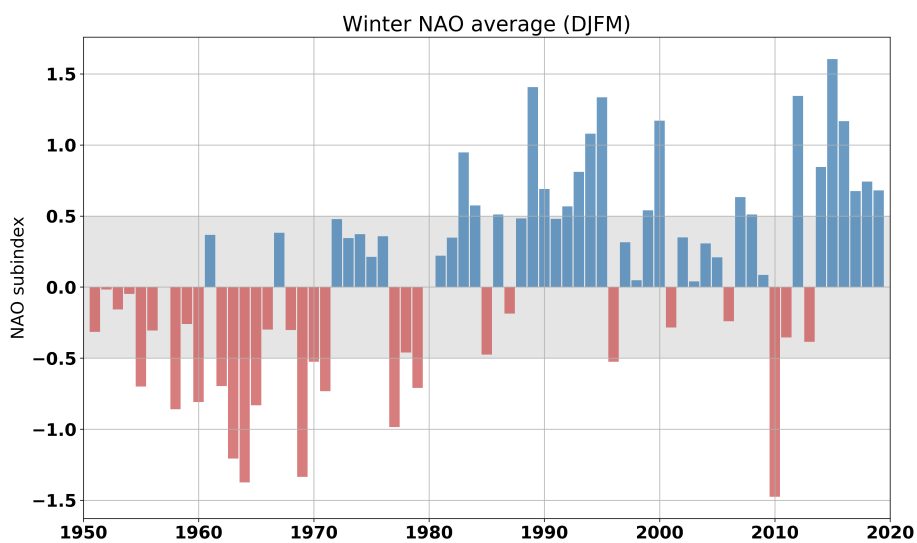
Figure 2. Winter North Atlantic Oscillation (NAO) index averaged over December to March. Here positive anomalies, generally indicative of colder conditions, are colored in blue. Shaded area correspond to ± 0.5 sd, indicating normal conditions. This time series is one component of the NL climate index.
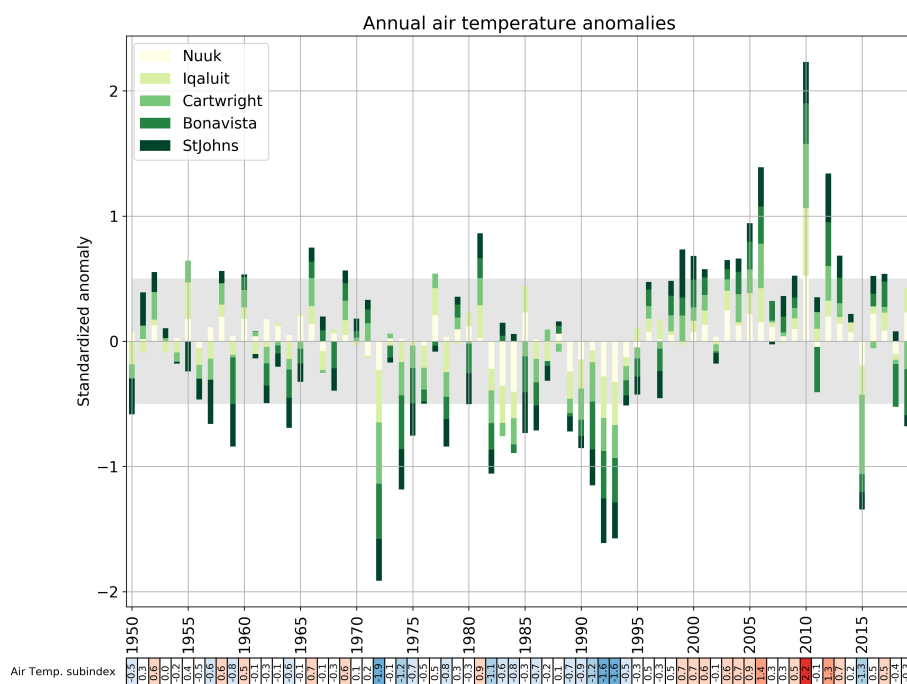
Figure 3. Normalized annual air temperature anomalies for Nuuk, Iqaluit, Cartwright, Bonavista and St. John's. This figure shows the average of the five stations, where the length of each bar correspond to the relative contribution of individual station to the average. The shaded area corresponds to the 1981-2010 average ± 0.5 sd. The numerical values of this time series are reported in a color-coded scorecards at the bottom of the figure. Positive anomalies (> 0.5 sd) are colored red, while negative anomalies (< -0.5 sd) are colored blue. In both cases, the darker the color, the stronger the anomaly. White corresponds to the climatological average ± 0.5 sd. This time series is one component of the NL climate index.
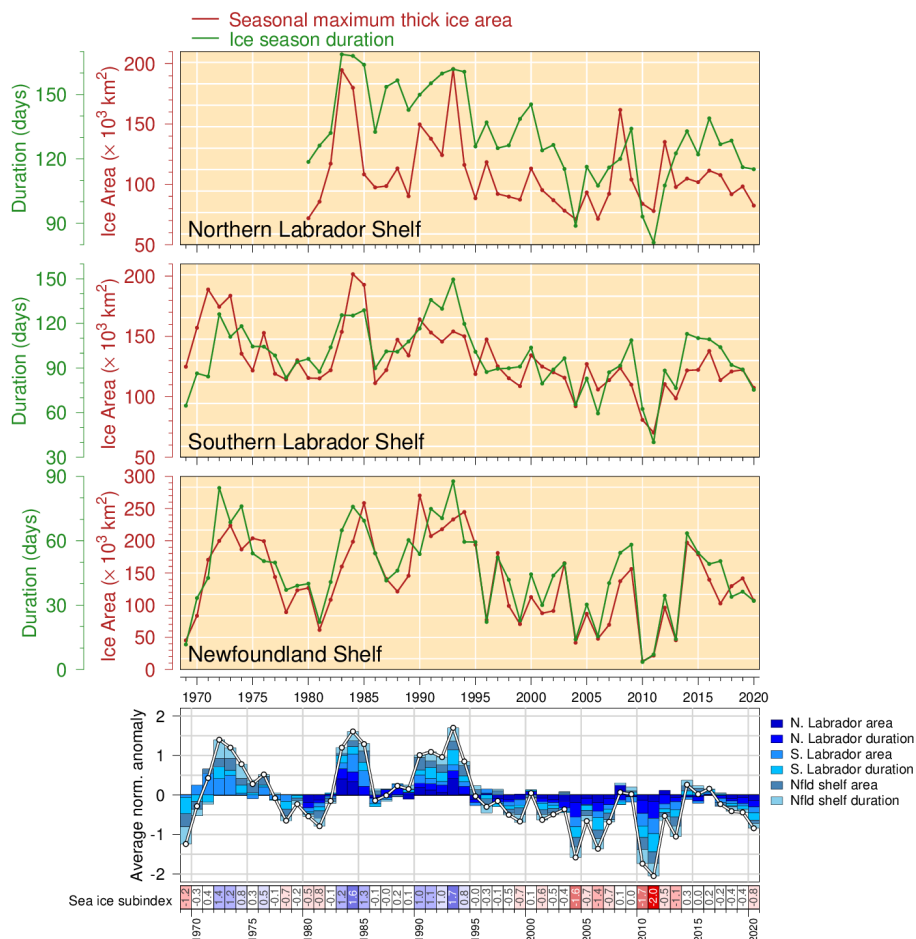
Figure 4. Sea ice season duration (green) and seasonal maximum area covered by thick ice (red) for Northern and Southern Labrador shelf (top two panels) and Newfoundland shelf (third panel). The Northern Labrador time series starts in 1980, while the two other start in 1969. The 6 time series are transformed into normalized anomalies and presented in a stacked bar fashion in the bottom panel. The scorecard at the bottom of this last panel presents the numerical values of the mean normalized anomalies for each year. Here negative anomalies (indicative of warmer conditions) are colored red and positive anomalies (colder conditions), blue. This time series is one component of the NL climate index.
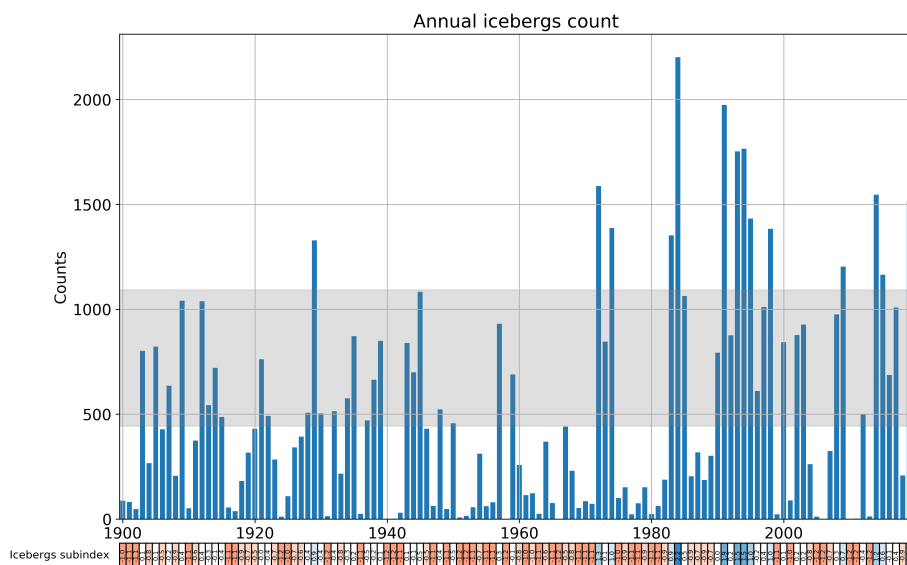
Figure 5. Annual iceberg count crossing south of 48°N on the northern Grand Bank. The shaded area corresponds to the 1981-2010 average ±0.5 sd. The normalized anomaly of this time series is provided below the main panel under the form of a color-coded scorecard. Here negative anomalies are red (generally corresponding to warmer conditions) and positive anomalies blue. This time series is one component of the NL climate index.
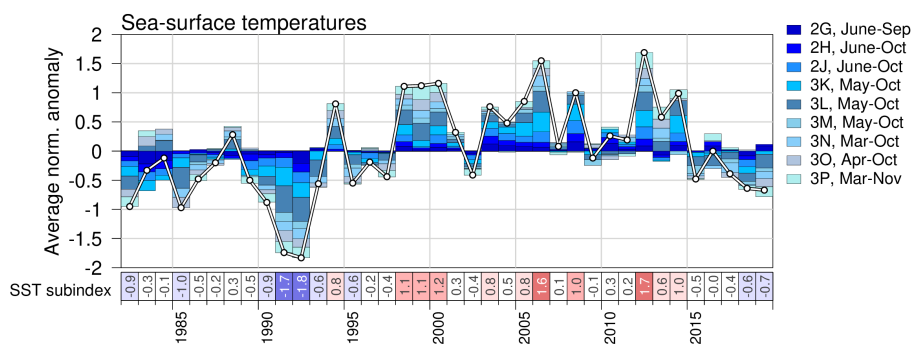
Figure 6. Sea Surface Temperature (SST) composite index in NAFO sub-areas 2 and 3 since 1982. This index is built by performing a spatially-weighted average of the seasonal SST normalized anomalies for each NAFO division (divisions and months used are provided on the right-and side of the figure). The numerical values of the normalized anomalies are provided in a color-coded (red, warm; blue, cold) scorecard at the bottom. This time series is one component of the NL climate index.
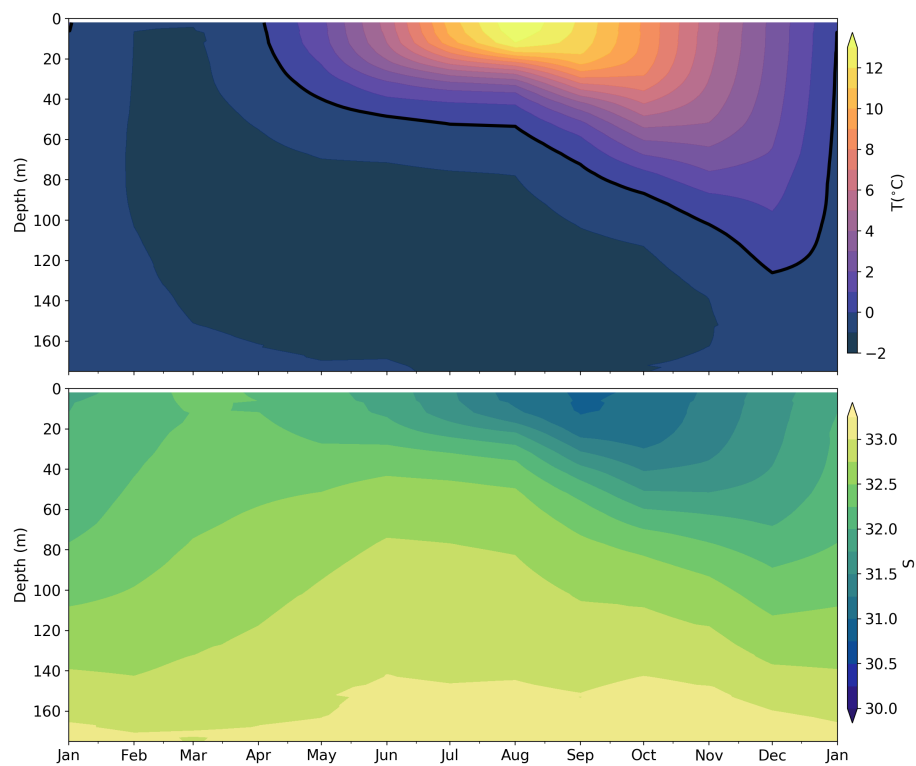
Figure 7. Climatological (1981-2010) annual cycle of temperature (top) and salinity (bottom) at Station 27. The thick black line in the top panel is the 0°C isotherm delimiting the top of the CIL.
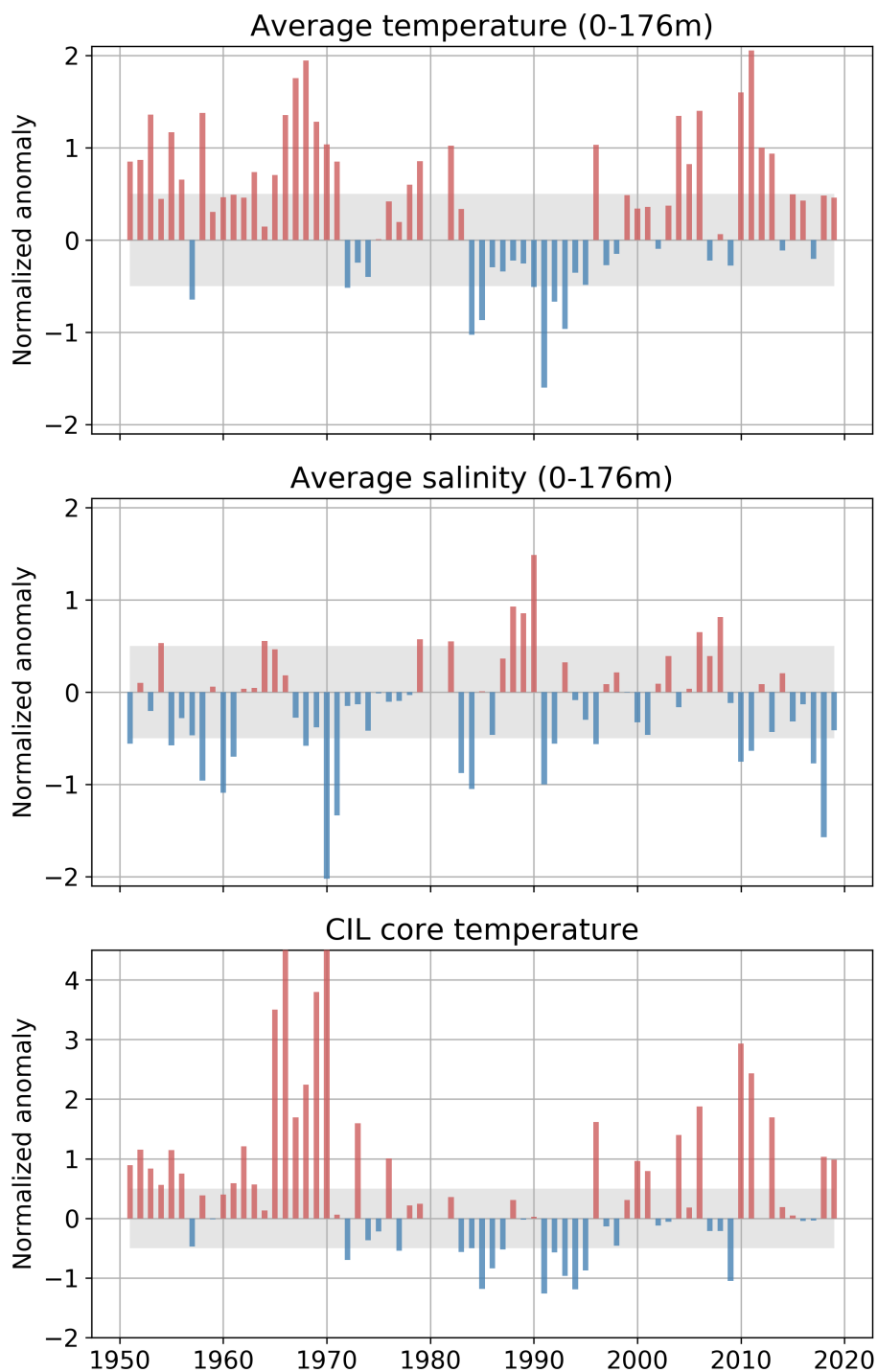
Figure 8. Normalized anomalies of the vertically averaged temperature (top) and salinity (center), and CIL core temperature (bottom) at Station 27. Shaded areas in all panels correspond to ±0.5 sd, indicating normal conditions. These three time series are components of the NL climate index.
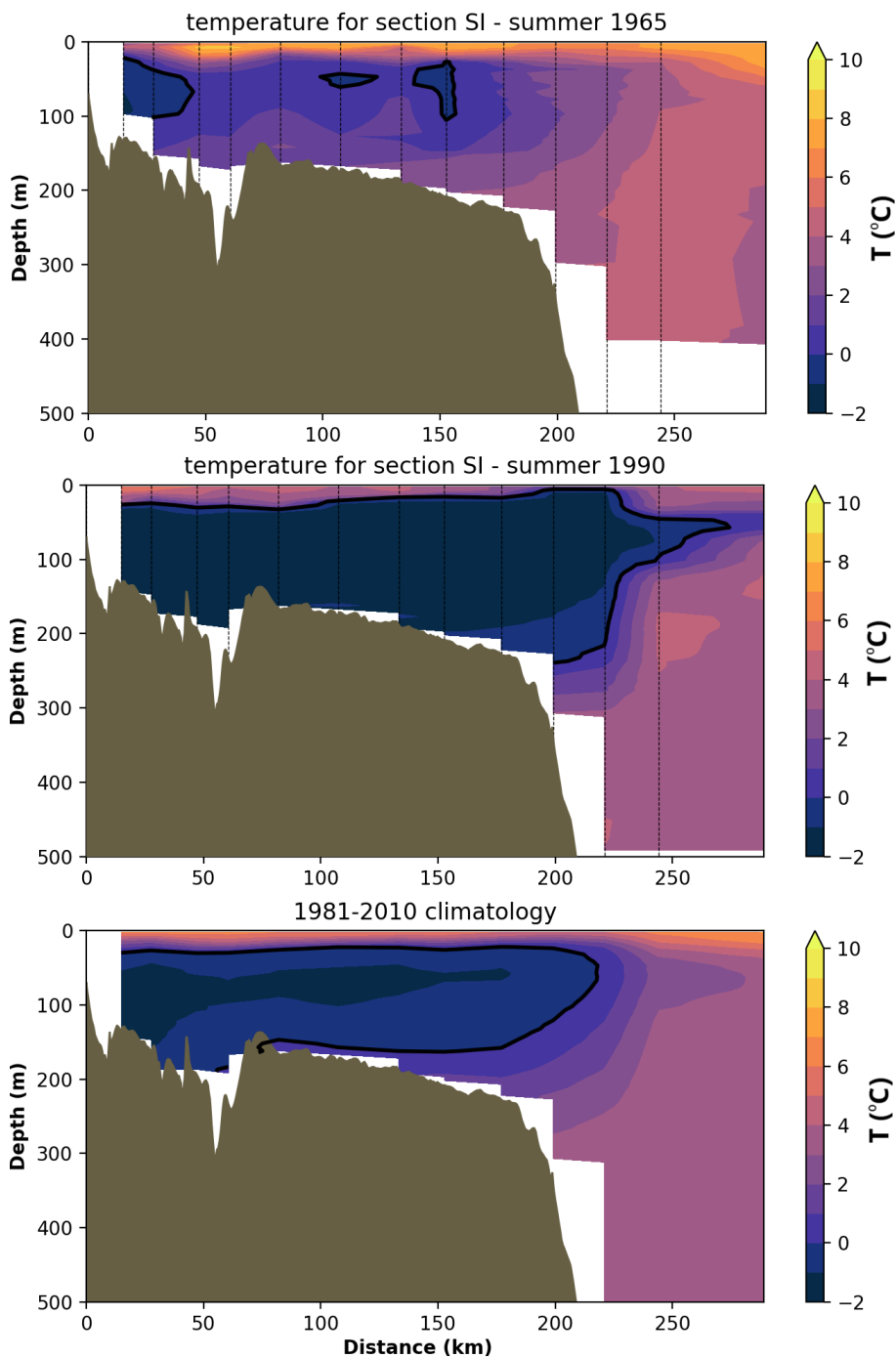
Figure 9. Summer temperature along hydrographic section Seal Island (SI) during 1965 (top), 1990 (center) and the 1981-2010 average (bottom). The vertical axis is limited to the top 500 m and the horizontal axis is the distance (in km) from the coast. The CIL (T<0°C) is highlighted with a thick black contour. Stations location are indicated with thin dashed lines.
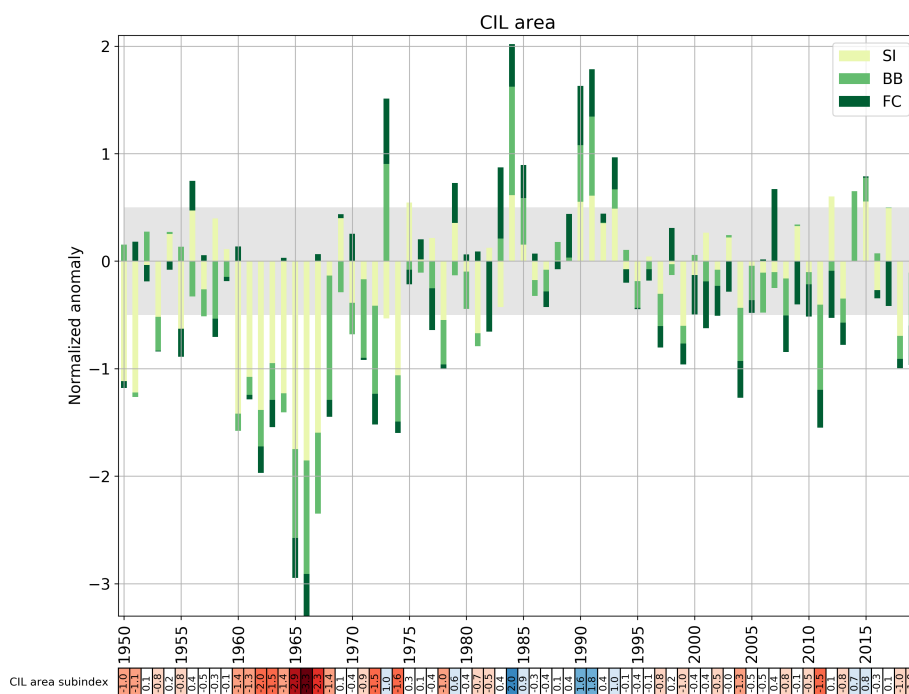
Figure 10. Normalized anomalies of the mean CIL area for hydrographic sections Seal Island (SI), Bonavista (BB) and Flemish Cap (FC). This time series correspond to the average of the 3 sections, where the contribution of each section is represented. The shaded area corresponds to the 1981-2010 average ±0.5 sd. The numerical values of this time series are reported in a color-coded scorecards at the bottom of the figure. Here negative anomalies (generally corresponding to warmer conditions) are colored red, and positive anomalies blue. This time series is one component of the NL climate index.
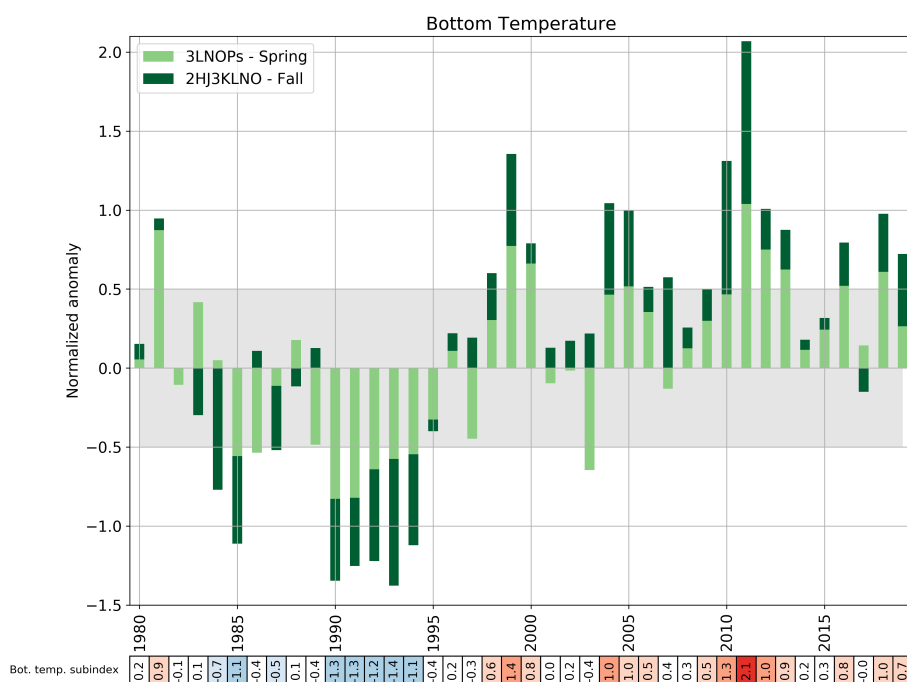
Figure 11. Normalized anomalies of bottom temperature in NAFO Dividions 3LNOPs (spring) and 2HJ3KLNO (fall). This time series corresponds to the average of the 2 seasons, where each contribution is represented. The shaded area corresponds to the 1981-2010 average ±0.5 sd. The numerical values of this time series are reported in a color-coded scorecards at the bottom of the figure. This time series is one component of the NL climate index.
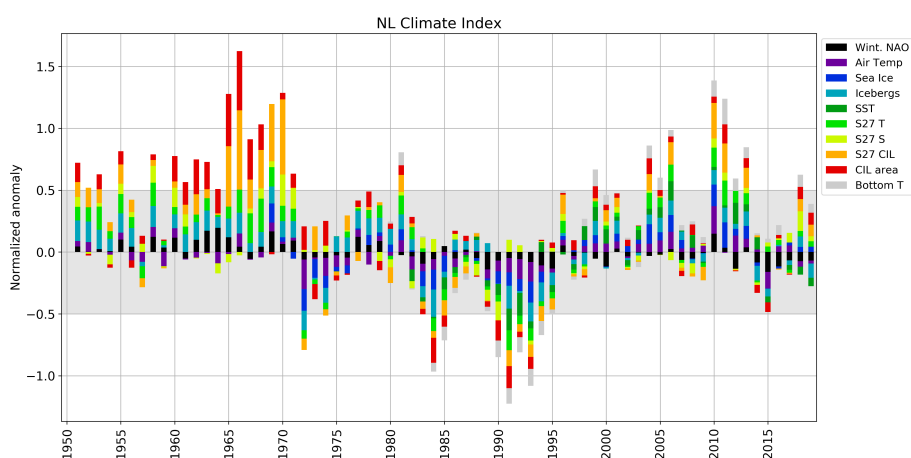
Figure 12. Figure to be updated; Newfoundland and Labrador climate index described in this study. The time series (which starts in 1951 unless specified) used for the climate index are the following: winter NAO index, the air temperature at 5 sites, the sea ice season duration and maximum area for the Northern Labrador, Southern Labrador and Newfoundland shelves (starts in 1969), the number of icebergs, SSTs in NAFO divisions 2GHJ3KLNOP (starts in 1982), vertically-averaged temperature and salinity at Station 27, CIL core temperature at Station 27, the summer CIL areas on the hydrographic sections Seal Island, Bonavista and Flemish Cap, and the spring and fall bottom temperature in NAFO divisions 3LNOPs and 2HJ3KLNO, respectively (starts in 1980). Some indices (NAO, ice, icebergs, salinity and CIL volume) have been reversed when positive anomalies are generally indicative of colder conditions.
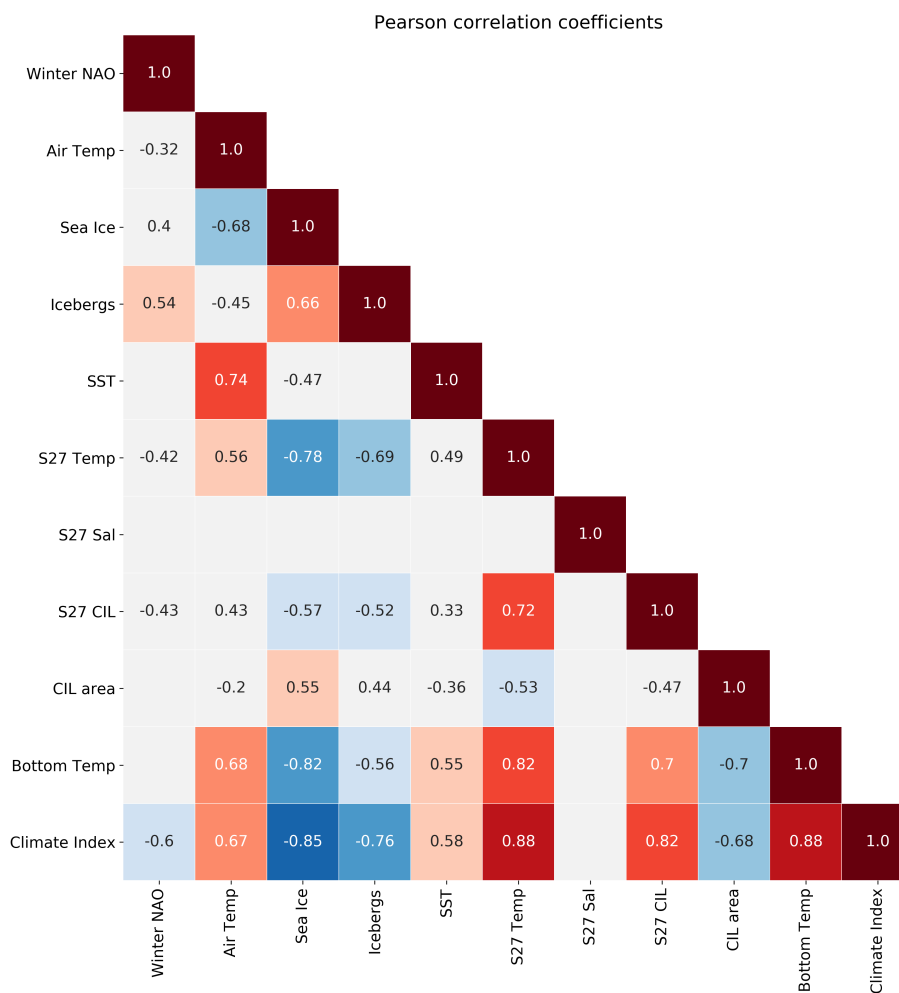
Figure 13. Pearson correlation (r) matrix between the different sub-indices of the NL climate index, and the NL climate index itself. Red and blue colors denote a positive and negative correlation, respectively. Only significant correlations (p-values < 0.05) are shown. Correlations less than ± 0.5 have been left white. The natural signs (not reversed) of the subindices have been used here in order to illustrate relationships in which positive (warm) anomalies in one variable (e.g., Station 27 temperature) is reflected by a negative anomalies in another (e.g., sea ice).
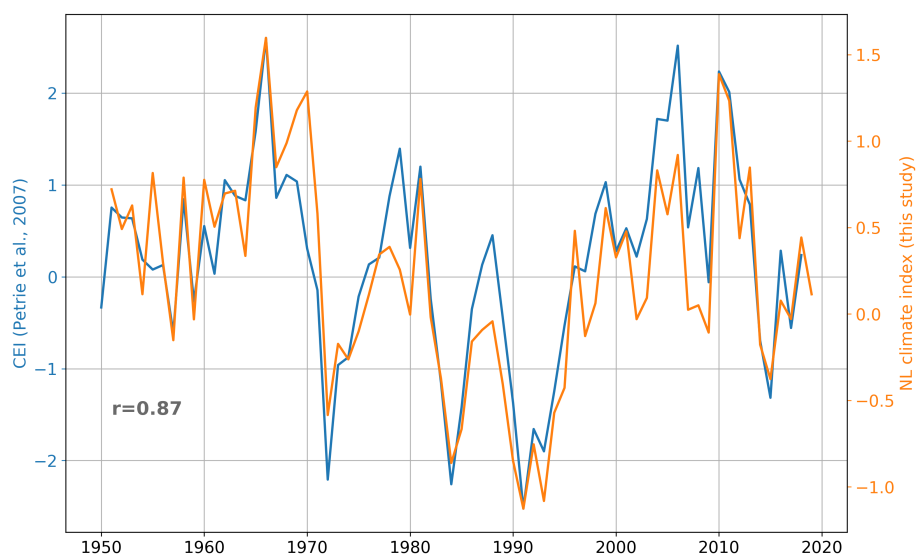
Figure 14. Comparison between the Composite Environmental Index (CEI) developed by Petrie et al. (2007) and used until recently (e.g. Cyr et al., 2019), and the new NL climate index introduced here. Note the difference vertical axis systems. The correlation between the two previous and the new indices is $r = 0.87$.